Applied Mathematics Letters 95 (2019) 122–129

Contents lists available at ScienceDirect

Applied Mathematics Letters

www.elsevier.com/locate/aml

A novel decoupled and stable scheme for an anisotropic phase-field dendritic crystal growth model

Jun Zhang [a,1], Chuanjun Chen [b,*,2], Xiaofeng Yang [c,3]

[a] *Computational Mathematics Research Center, Guizhou University of Finance and Economics, Guiyang 550025, China*
[b] *School of Mathematics and Information Sciences, Yantai University, Yantai 264005, China*
[c] *Department of Mathematics, University of South Carolina, Columbia, SC 29208, United States*

ARTICLE INFO

Article history:
Received 8 March 2019
Received in revised form 25 March 2019
Accepted 25 March 2019
Available online 3 April 2019

Keywords:
Phase-field
Dendritic
Stabilized-IEQ
Anisotropy
Decoupled

ABSTRACT

We consider numerical approximations for a phase-field dendritic crystal growth model, which is a highly nonlinear system that couples the anisotropic Allen–Cahn type equation and the heat equation. By combining the stabilized-Invariant Energy Quadratization method with a novel decoupling technique, the scheme requires solving only a sequence of linear elliptic equations at each time step, making it the first, to the best of the author's knowledge, totally decoupled, linear, unconditionally energy stable scheme for the model. We further prove the unconditional energy stability rigorously and present various numerical simulations to demonstrate the stability and accuracy.

1. Introduction

In this paper, we consider numerical approximations for a phase-field dendritic crystal growth model which was proposed in [1], where the system is composed of two second-order, coupled nonlinear equations: the Allen–Cahn type equation with a gradient-dependent anisotropic coefficient, and the heat transfer equation. The phase-field method had been widely used in the modeling and numerical simulations for investigating the process of dendritic crystal growth since the pioneering modeling work of Halperin, Kobayashi, and Collins et al. in [2–4], and some subsequent modeling/simulation advances in [5–10].

While it might be easy to design energy stable schemes to solving the coupled nonlinear phase-field systems at each time step, it is extremely difficult to construct decoupled, and preferably linear, elliptic

* Corresponding author.
E-mail addresses: jzhang@mail.gufe.edu.cn (J. Zhang), cjchen@ytu.edu.cn (C. Chen), xfyang@math.sc.edu (X. Yang).

[1] J. Zhang was partially supported by the Science Technology Foundation of Guizhou Educational Department (No. QJK[KY],[2019]1051).
[2] C. Chen was partially supported by NSFC, China-11771375, 11571297, and Shandong Province Natural Science Foundation ZR2018MAQ008.
[3] X. Yang was partially supported by NSF-DMS-1720212 and DMS-1818783.

https://doi.org/10.1016/j.aml.2019.03.029
0893-9659/

equations while preserving the energy stability. For the particular dendritic model proposed in [1], the main numerical challenges include: (i) the stiffness of the phase equation associated with the interfacial width; (ii) the anisotropic coefficient which induces large spatial oscillations that may cause the computations easily blow up or loss of accuracy; and (iii) the coupling between the temperature and phase function through the nonlinear latent heat transfer terms. We recall that the difficulty (i) had been studied extensively and some methods have been proved to be effective, cf. [11–18]. However, for the difficulty (ii) and (iii), most of the available schemes are either coupled nonlinear which need some efficient iterative solvers, and/or do not preserve energy stability at all, see [19–22]. Hence, thus far, it remains unclear on how to construct a *decoupled* scheme while keeping the other two desirable features: unconditionally energy stable and linear.

The aim of this paper is to construct an efficient scheme with these features mentioned above for solving the coupled nonlinear phase-field dendritic model. To this end, we develop a novel decoupling technique, where an extra stabilizing term is added to the latent heat transfer term, and combine it with the stabilized-IEQ approach developed in [23–25], to construct a totally decoupled time discretization scheme, which leads to, at each time step, an elliptic system for the phase function, and a linear elliptic equation for the temperature. We rigorously prove that the scheme is unconditionally energy stable. *To the best of author's knowledge, the scheme is the first totally decoupled, linear, unconditionally energy stable scheme for the phase-field dendritic crystal growth model.*

The remaining of the paper is organized as follows. In Section 2, we give a brief introduction of the governing PDE system for the phase-field anisotropic dendritic crystal growth model. In Section 3, we develop a numerical scheme for solving the model, and rigorously prove its unconditional energy stability. Various numerical experiments are given in Section 4 to demonstrate the accuracy and efficiency of the proposed numerical scheme. Finally, some concluding remarks are given in Section 5.

2. Model equations

We give a brief description of the anisotropic phase-field dendritic crystal growth model proposed in [1]. Let Ω be a smooth, open, bounded, connected domain in $\mathbb{R}^d$ with $d = 2, 3$. A scalar phase-field function $\phi(\boldsymbol{x}, t)$ is introduced to label the liquid and solid phases, where $\phi = 1$ for the solid and $\phi = -1$ for the fluid. These two regions are connected by a smooth transitional layer with the thickness ϵ. The total effective free energy is postulated as follows,

$$E(\phi, T) = \int_\Omega \Big(\frac{1}{2} |\kappa(\nabla\phi)\nabla\phi|^2 + \frac{\lambda}{2\epsilon K} T^2 + \frac{1}{4\epsilon^2} F(\phi) \Big) d\boldsymbol{x}, \tag{2.1}$$

in which, $T(\boldsymbol{x}, t)$ is the temperature, ϵ, λ and K are all positive parameters, $F(\phi) = (\phi^2 - 1)^2$ is the Ginzburg–Landau double well potential, $\kappa(\nabla\phi)$ is a function describing the anisotropic property that depends on the direction of the outer normal vector $\boldsymbol{n}$ which is the interface normal defined as $\boldsymbol{n} = -\frac{\nabla\phi}{|\nabla\phi|}$. For the 2D system, the anisotropy coefficient $\kappa(\nabla\phi)$ is usually given by

$$\kappa(\nabla\phi) = 1 + \epsilon_4 \cos(m\theta), \tag{2.2}$$

where m is the number of folds of anisotropy, ϵ_4 is the parameter for the anisotropy strength, and $\theta = \arctan(\frac{\phi_y}{\phi_x})$. By adopting the L^2-gradient flow relaxation dynamics for the dendritic crystal growth, one obtains the governing dynamical equations via the variational approach, which reads as follows:

$$\tau(\phi)\phi_t = \nabla \cdot (\kappa^2(\nabla\phi)\nabla\phi + \kappa(\nabla\phi)|\nabla\phi|^2 \boldsymbol{H}(\phi)) - \frac{f(\phi)}{\epsilon^2} - \frac{\lambda}{\epsilon} p'(\phi) T, \tag{2.3}$$

$$T_t = D\Delta T + K p'(\phi)\phi_t, \tag{2.4}$$

where, $\tau(\phi) > 0$ is the mobility parameter that is chosen either as a constant [1,26] or a function of ϕ [1], D is the diffusion rate of the temperature, $\boldsymbol{H}(\phi)$ in 2D reads as

$$\boldsymbol{H}(\phi) = \frac{\delta\kappa(\nabla\phi)}{\delta\phi} = 4\varepsilon_4 \frac{4}{|\nabla\phi|^6}\Big(\phi_x(\phi_x^2\phi_y^2 - \phi_y^4),\ \phi_y(\phi_x^2\phi_y^2 - \phi_x^4)\Big), \tag{2.5}$$

the function $p(\phi)$ accounting for the generation of latent heat is a phenomenological functional taking the form preserving the minima of ϕ at ± 1 independently of the local value of T. The common choice for $p(\phi)$ is $p(\phi) = \frac{1}{5}\phi^5 - \frac{2}{3}\phi^3 + \phi$ and $p'(\phi) = (1-\phi^2)^2$ that implies the heat only transfers through the interface [1,3]. Without the loss of generality, we adopt the periodic boundary condition in this study to remove the complexities from the boundary integrals.

3. Numerical schemes

The aim of this section is to construct a totally decoupled, energy stable scheme to solving the system (2.3)–(2.4). To realize the linear and unconditionally energy stable features, we handle the nonlinear anisotropic gradient potential and the double-well potential by adopting the stabilized-IEQ approach developed in [23]. To realize the decoupling feature, we develop a novel decoupling technique by introducing an intermediate temperature that combines the temperature at previous time step and an extra semi-explicit stabilizing term. Finally, a decoupled and linear scheme is obtained and it can be proved to be unconditionally energy stable theoretically and numerically.

We define an auxiliary variable $U(\boldsymbol{x}, t)$ that reads as follows:

$$U = \sqrt{\frac{1}{2}|\kappa(\nabla\phi)\nabla\phi|^2 + \frac{1}{4\epsilon^2}F(\phi) + B}, \tag{3.1}$$

where B is a constant that can ensure the radicand positive. By taking the time derivative of the new variable U, we then reformulate the system (2.3)–(2.4) as the following equivalent PDE system,

$$\tau(\phi)\phi_t = -Z(\phi)U - \frac{\lambda}{\epsilon}p'(\phi)T, \tag{3.2}$$

$$U_t = \frac{1}{2}Z(\phi)\phi_t, \tag{3.3}$$

$$T_t = D\Delta T + Kp'(\phi)\phi_t, \tag{3.4}$$

where

$$Z(\phi) = \frac{-\nabla\cdot(\kappa^2(\nabla\phi)\nabla\phi + \kappa(\nabla\phi)|\nabla\phi|^2\boldsymbol{H}(\phi)) + \frac{1}{\epsilon^2}f(\phi)}{\sqrt{\frac{1}{2}|\kappa(\nabla\phi)\nabla\phi|^2 + \frac{1}{4\epsilon^2}F(\phi) + B}}. \tag{3.5}$$

The initial conditions are given by

$$\begin{cases} \phi(t=0) = \phi_0,\ T(t=0) = T_0, \\ U(t=0) = \sqrt{\frac{1}{2}|\kappa(\nabla\phi_0)\nabla\phi_0|^2 + \frac{1}{4\epsilon^2}F(\phi_0) + B}. \end{cases} \tag{3.6}$$

The boundary conditions are still periodic that we alluded before.

Next, we will develop an energy stable time marching algorithm for solving the transformed system (3.2)–(3.4). Let $\delta t > 0$ be a time step size and set $t^n = n\delta t$ for $0 \le n \le N$ with $t_{max} = N\delta t$. ψ^n denotes the numerical approximation to $\psi(\cdot, t)|_{t=t^n}$ for any function ψ. We construct a first-order time marching scheme for solving the system (3.2)–(3.4) based on the first-order backward formula, shown as follows.

Assuming ϕ^n, U^n, T^n are known, we update $\phi^{n+1}, U^{n+1}, T^{n+1}$ by solving the following scheme.

Step 1:

$$\tau(\phi^n)\frac{\phi^{n+1}-\phi^n}{\delta t}+\frac{S_1}{\epsilon^2}(\phi^{n+1}-\phi^n)-S_2\Delta(\phi^{n+1}-\phi^n)=-Z^nU^{n+1}-\frac{\lambda}{\epsilon}p'(\phi^n)T_\star^n, \tag{3.7}$$

$$\frac{T_\star^n-T^n}{\delta t}=Kp'(\phi^n)\frac{\phi^{n+1}-\phi^n}{\delta t}, \tag{3.8}$$

$$U^{n+1}-U^n=\frac{1}{2}Z^n(\phi^{n+1}-\phi^n), \tag{3.9}$$

where $Z^n=Z(\phi^n)$ and S_i, $i=1,2$ are two positive stabilizing parameters.

Step 2:

$$\frac{T^{n+1}-T_\star^n}{\delta t}-D\Delta T^{n+1}=0. \tag{3.10}$$

Remark 3.1. The scheme (3.7)–(3.10) is a totally decoupled, linear scheme by using the intermediate temperature $T_\star^n$ and the implicit–explicit discretization for the nonlinear terms. (3.8) implies that $T_\star^n$ is a first-order approximation to T^n. Moreover, from (3.8), the heat transfer term is already included in the intermediate temperature $T_\star^n$, hence this term vanishes in the heat equation (3.10) as a result.

It is remarkable that the intermediate variable $T_\star^{n+1}$ and the new variable U^{n+1} will not bring up any extra computational costs. Indeed, (3.7)–(3.9), and (3.10) are respectively (decoupled) linear elliptic equations for ϕ^{n+1} and T^{n+1}. This is because we can rewrite (3.10) as follows

$$U^{n+1}=\frac{1}{2}Z^n\phi^{n+1}+A_1, \tag{3.11}$$

where $A_1=U^n-\frac{1}{2}Z^n\phi^n$. Then, by substituting (3.11) and (3.8) to (3.7), the system (3.7)–(3.9) can be rewritten as

$$\mathscr{L}(\phi^{n+1})=f, \tag{3.12}$$

where

$$\begin{cases}\mathscr{L}(\psi)=\dfrac{1}{\delta t}\tau(\phi^n)\psi+\dfrac{S_1}{\epsilon^2}\psi-S_2\Delta\psi+\dfrac{1}{2}Z^nZ^n\psi+\dfrac{\lambda K}{\epsilon}p'(\phi^n)p'(\phi^n)\psi,\\ f=\tau(\phi^n)\dfrac{\phi^n}{\delta t}+\dfrac{S_1}{\epsilon^2}-S_2\Delta\phi^n-Z^nA_1-\dfrac{\lambda}{\epsilon}p'(\phi^n)(T^n-Kp'(\phi^n)\phi^n).\end{cases} \tag{3.13}$$

In practice, we first solve the linear system (3.12) directly to obtain ϕ^{n+1}, and then update the variables $T_\star^{n+1}$ and U^{n+1} from (3.8) and (3.11). Therefore, at each time step, one only needs to solve a sequence of decoupled elliptic equations which can be solved very efficiently. We can further prove the linear system is well-posed from the Lax–Milgram theorem but omit the details due to the page limit.

Now we prove the scheme (3.7)–(3.10) is unconditionally energy stable as follows.

Theorem 3.1. *The scheme (3.7)–(3.10) is unconditionally energy stable which satisfies the following discrete energy dissipation law,*

$$\frac{1}{\delta t}(E^{n+1}-E^n)\le-\|\sqrt{\tau(\phi^n)}\frac{\phi^{n+1}-\phi^n}{\delta t}\|^2-\frac{\lambda D}{\epsilon K}\|\nabla T^{n+1}\|^2\le 0, \tag{3.14}$$

where $E^{n+1}=\int_\Omega(|U^{n+1}|^2+\frac{\lambda}{2\epsilon K}|T^{n+1}|^2-B)d\boldsymbol{x}$.

Proof. By taking the L^2 inner product of (3.7) with $\phi^{n+1}-\phi^n$, and using the identity

$$2(a-b)a=a^2-b^2+(a-b)^2,$$

we obtain

$$\begin{aligned}\delta t\left\|\sqrt{\tau(\phi^n)}\frac{\phi^{n+1}-\phi^n}{\delta t}\right\|^2+\frac{S_1}{\epsilon^2}\|\phi^{n+1}-\phi^n\|^2+S_2\|\nabla(\phi^{n+1}-\phi^n)\|^2\\ =-(Z^nU^{n+1},\phi^{n+1}-\phi^n)-\frac{\lambda}{\epsilon}(p'(\phi^n)T^n_\star,\phi^{n+1}-\phi^n).\end{aligned}\tag{3.15}$$

By taking the L^2 inner product of (3.8) with $\frac{\lambda}{\epsilon K}\delta t T^n_\star$, we obtain

$$\frac{\lambda}{2\epsilon K}(\|T^n_\star\|^2-\|T^n\|^2+\|T^n_\star-T^n\|^2)=\frac{\lambda}{\epsilon}(p'(\phi^n)(\phi^{n+1}-\phi^n),T^n_\star).\tag{3.16}$$

By taking the L^2 inner product of (3.9) with $2U^{n+1}$, we obtain

$$\|U^{n+1}\|^2-\|U^n\|^2+\|U^{n+1}-U^n\|^2=(Z^n(\phi^{n+1}-\phi^n),U^{n+1}).\tag{3.17}$$

By taking the L^2 inner product of (3.10) with $\frac{\lambda}{\epsilon K}\delta t T^{n+1}$, we obtain

$$\frac{\lambda}{2\epsilon K}(\|T^{n+1}\|^2-\|T^n_\star\|^2+\|T^{n+1}-T^{n-1}_\star\|^2)=\frac{\lambda D}{\epsilon K}\delta t\|\nabla T^{n+1}\|^2.\tag{3.18}$$

By combining (3.15), (3.16), (3.17), and (3.18), we obtain

$$\begin{aligned}&\|U^{n+1}\|^2-\|U^n\|^2+\frac{\lambda}{2\epsilon K}(\|T^{n+1}\|^2-\|T^n\|^2)\\ &\quad+\frac{\lambda}{2\epsilon K}(\|T^n_\star-T^n\|^2+\|T^{n+1}-T^n_\star\|^2)+\|U^{n+1}-U^n\|^2\\ &\quad+\frac{S_1}{\epsilon^2}\|\phi^{n+1}-\phi^n\|^2+S_2\|\nabla(\phi^{n+1}-\phi^n)\|^2=-\delta t\left\|\sqrt{\tau(\phi^n)}\frac{\phi^{n+1}-\phi^n}{\delta t}\right\|^2-\frac{\lambda D}{\epsilon K}\delta t\|\nabla T^{n+1}\|^2.\end{aligned}$$

Finally, we obtain the desired result after dropping some positive terms. □

Remark 3.2. Note the energy laws is based on the modified energy in terms of the new defined variable U. For the continuous case, the energy law for the transformed system (3.2)–(3.4) is exactly the same as the energy law for the original system (2.3)–(2.4). For the discrete case, the modified energy is an approximation to the original energy with the first-order accuracy.

4. Numerical simulations

In this section, we present various numerical examples to demonstrate accuracy, energy stability, and efficiency of the proposed scheme.

4.1. Accuracy test

We first implement a numerical example with fourfold anisotropy ($m=4$) in 2D space $\Omega=[0,2\pi]\times[0,2\pi]$ to test the convergence rates of the proposed scheme (3.7)–(3.10), denoted by S-IEQ. To show the accuracy comparisons, we also compute the convergence rates by using the non-stabilized version, i.e., scheme (3.7)–(3.10) but with $S_1=S_2=0$, denoted by IEQ.

We assume the following two functions

$$\phi(x,y,t)=\sin(x)\cos(y)\cos(t),\ T(x,y,t)=\cos(x)\sin(y)\cos(t)\tag{4.1}$$

to be the exact solutions, and impose some suitable force fields such that the given solutions can satisfy the system (2.3)–(2.4). The model parameters are set as follows,

$$\tau(\phi)=\tau_0,\epsilon=0.06,\epsilon_4=0.05,D=\lambda=K=1,S_1=S_2=4,B=1\text{e}5.$$

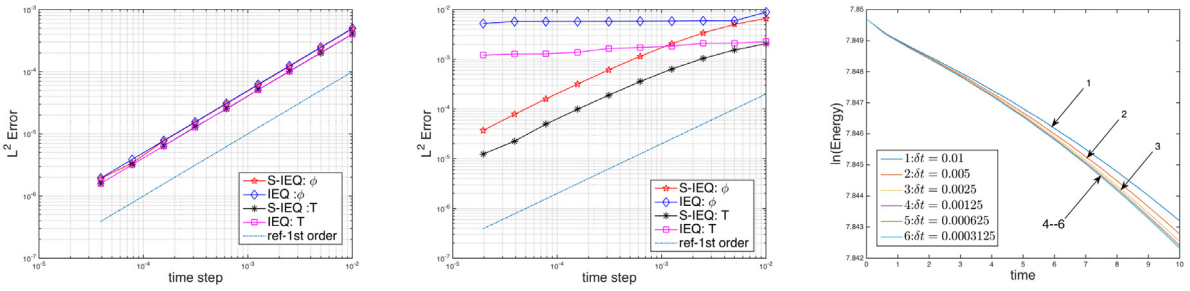

Fig. 4.1. The L^2 numerical errors for the phase variable ϕ and temperature T at $t = 0.2$ with the mobility parameter (a) $\tau_0 = \frac{1}{\epsilon^2}$ and (b) $\tau_0 = \frac{1}{\epsilon}$ and various time steps. (c) Time evolutions of the logarithm of the total energy (2.1) computed by six different time step sizes until $t = 10$.

We discretize the space by using $N_x = N_y = 129$ Fourier modes for x and y directions so that the errors from the spatial discretization are negligible compared to the temporal discretization errors.

In Fig. 4.1(a), we set $\tau_0 = \frac{1}{\epsilon^2}$ and plot the errors computed by using the two schemes, S-IEQ and IEQ. We observe these two schemes not only present the good convergence rate that almost perfectly matches the first-order accuracy for the time step but also good approximations to the exact solution, regardless of whether they are stabilized or not. In Fig. 4.1(b), we set $\tau_0 = \frac{1}{\epsilon}$. We observe that the non-stabilized scheme IEQ totally loses the accuracy for all tested time steps. On the contrary, the scheme S-IEQ is stable for all tested time steps and perform good approximations and the first-order accuracy all along. Therefore, we conclude that (i) if the mobility parameter τ_0 is large, both schemes can solve the model well; and (ii) if the mobility parameter τ_0 is small, the stabilized scheme S-IEQ overwhelmingly defeats its non-stabilized version IEQ from the stability and/or accuracy. In Fig. 4.1(c), we plot the evolution curves of the total energy (2.1) computed by six different time step sizes until $t = 10$. For all tested time steps, the obtained energy curves show the monotonic decays that confirm the developed algorithm is unconditionally stable.

4.2. 2D dendrite crystal growth with sixfold anisotropy

In this subsection, we investigate the dynamics on how the anisotropic coefficient affects the shape of the dendritic crystal. We initially deposit a single small crystal nucleus in the center of the computed domain and observe how it grows heterogeneously. This is a benchmark simulation that had been extensively studied in [1,3,9,27].

The initial condition reads as

$$\begin{cases} \phi(x,y,t=0) = \tanh\left(\dfrac{r_0 - \sqrt{(x-x_0)^2 + (y-y_0)^2}}{\epsilon_0}\right); \\ T(x,y,t=0) = \begin{cases} 0, & \phi > 0; \\ T_0, & \text{otherwise}, \end{cases} \end{cases} \tag{4.2}$$

where $(x_0, y_0, r_0, \epsilon_0, T_0) = (\pi, \pi, 0.02, 0.072, -0.55)$, and the model parameters read as follows,

$$\tau = 4.4\text{e}3, \epsilon = 1.12\text{e}{-2}, \epsilon_4 = 0.05, D = 2.25\text{e}{-4}, K = 0.5, \lambda = 380, S_1 = S_2 = 4, B = 1\text{e}5. \tag{4.3}$$

We discretize the space using $N_x = N_y = 513$ Fourier modes.

We investigate the sixfold ($m = 6$) anisotropic case by varying the parameter K and fixing all other parameters from (4.3). We summarize the contour of the interface $\{\phi = 0\}$ every 20 time units from the initial moment in Fig. 4.2 for three cases of $K = 0.65$, $K = 0.7$ and $K = 0.75$. We observe that circular nucleus grows into various snow-flake patterns but always with six sub-branches. These simulations are qualitatively consistent with [3] where a slightly different model was used.

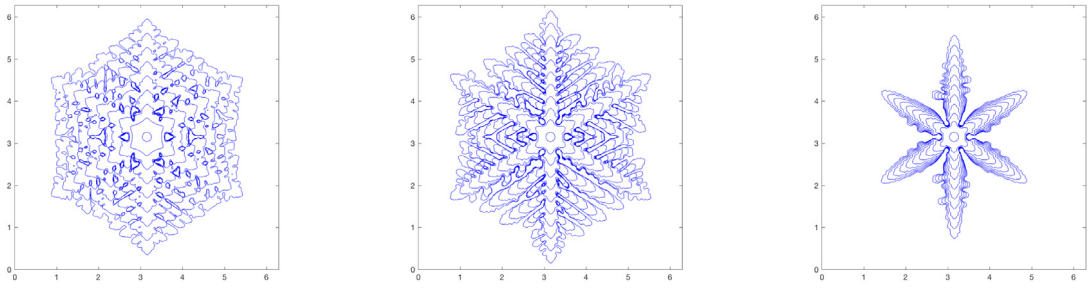

(a) $K = 0.65$. (b) $K = 0.7$. (c) $K = 0.75$.

Fig. 4.2. The summary of the contour of the interface $\{\phi = 0\}$ every 20 time units from the initial moment for the sixfold anisotropy by using the four different parameters K, where, (a) $K = 0.65$, (b) $K = 0.7$, and (c) $K = 0.75$.

5. Concluding remarks

In this paper, we have developed a totally decoupled, linear, and unconditionally energy stable scheme for solving the anisotropic dendritic phase-field model. Compared to the existing schemes for the anisotropic model, the proposed decoupled schemes (i) conquer the inconvenience from nonlinearities by linearizing the nonlinear terms in a new way, (ii) possess advantages of easy implementations and lower computational cost, (iii) are provably and/or numerically unconditionally energy stable, and thus (iv) allow for large time steps in computations. The technique developed in this paper can be used to construct efficient numerical schemes in other situations, for example, the dendritic solidification phase-field model with melt convection [28], or the binary alloy solidification model [29].

References

[1] A. Karma, W. Rappel, Phase-field model of dendritic sidebranching with thermal noise, Phys. Rev. E 60 (1999) 3614–3625.
[2] J.B. Collins, H. Levine, Diffuse interface model of diffusion-limited crystal growth, Phys. Rev. B 31 (1985) 6119–6122.
[3] R. Kobayashi, Modeling and numerical simulations of dendritic crystal growth, Physica D 63 (1993) 410.
[4] B.I. Halperin, P.C. Hohenberg, S.-K. Ma, Renormalization-group methods for critical dynamics: I. recursion relations and effects of energy conservation, Phys. Rev. B 139 (1974) 10.
[5] C.C. Chen, Y.L. Tsai, C.W. Lan, Adaptive phase field simulation of dendritic crystal growth in a forced flow:2d vs. 3d morphologies, Int. J. Heat Mass Transfer 52 (2009) 1158–1166.
[6] A. Karma, W. Rappel, Quantitative phase-field modeling of dendritic growth in two and three dimensions, Phys. Rev. E 57 (1998) 4323–4349.
[7] M. Plapp, A. Karma, Multiscale finite-difference-diffusion-monte-carlo method for simulating dendritic solidification, J. Comput. Phys. 165 (2000) 592–619.
[8] A. Shah, A. Haider, S. Shah, Numerical simulation of two dimensional dendritic growth using phase field model, World J. Mech. 4 (2014) 128–136.
[9] A. Karma, A.E. Lobkovsky, Unsteady crack motion and branching in a phase-field model of brittle fracture, Phys. Rev. Lett. 92 (2004) 245510.
[10] J. Li, J. Zhao, Q. Wang, Energy and entropy preserving numerical approximations of thermodynamically consistent crystal growth models, J. Comput. Phys. 382 (2019) 202–220.
[11] D.J. Eyre, Unconditionally gradient stable time marching the Cahn-Hilliard equation, in: Computational and Mathematical Models of Microstructural Evolution (San Francisco, CA, 1998), in: Mater. Res. Soc. Sympos. Proc., vol. 529, 1998, pp. 39–46.
[12] J. Shen, X. Yang, Numerical approximations of Allen-Cahn and Cahn-Hilliard equations, Disc. Conti. Dyn. Sys.-A 28 (2010) 1669–1691.
[13] J. Shen, X. Yang, A phase-field model and its numerical approximation for two-phase incompressible flows with different densities and viscositites, SIAM J. Sci. Comput. 32 (2010) 1159–1179.
[14] C. Xu, T. Tang, Stability analysis of large time-stepping methods for epitaxial growth models, SIAM. J. Num. Anal. 44 (2006) 1759–1779.
[15] X. Yang, Linear, first and second order and unconditionally energy stable numerical schemes for the phase field model of homopolymer blends, J. Comput. Phys. 327 (2016) 294–316.

[16] H. Gomez, T.J.R. Hughes, Provably unconditionally stable, second-order time-accurate, mixed variational methods for phase-field models, J. Comput. Phys. 230 (2011) 5310–5327.
[17] H. Gomez, der Zee Van, G. Kristoffer, Computational phase-field modeling, in: Encyclopedia of Computational Mechanics, second ed., John Wiley & Sons, Ltd, ISBN: 978-1-119-00379-3, 2017.
[18] I. Romero, Thermodynamically consistent time stepping algorithms for nonlinear thermomechanical systems, Internat. J. Numer. Methods Engrg. 79 (2009) 706–732.
[19] J.C. Ramirez, C. Beckermann, A. Karma, H.-J. Diepers, Phase-field modeling of binary alloy solidication with coupled heat and solute diffusion, Phys. Rev. E 69 (2004) 051607.
[20] N. Provatas, N. Goldenfeld, J. Dantzig, Efficient computation of dendritic microstructures using adaptive mesh refinement, Phys. Rev. Lett. 80 (1998) 3308–3311.
[21] B. Nestler, D. Danilov, P. Galenko, Crystal growth of pure substances: phase field simulations in comparison with analytical and experimental results, J. Comput. Phys. 207 (2005) 221–239.
[22] Y. Li, J. Kim, Phase-field simulations of crystal growth with adaptive mesh refinement, Inter. J. Heat. Mass. Trans. 55 (2012) 7926–7932.
[23] X. Yang. Efficient Linear, stabilized, Second order time marching schemes for an anisotropic phase field dendrtic crystal growth model, Comput. Meth. Appl. Mech. Engrg. 347 (2019) 316–339.
[24] C. Chen, X. Yang, Efficient numerical scheme for a dendritic solidification phase field model with melt convection, J. Comput. Phys. 388 (2019) 41–62.
[25] Z. Xu, X. Yand, H. Zhang, Z. Xie, Efficient and linear schemes for anisotropic Cahn-Hilliard model using the stabilized-invariant energy quadratization (S-IEQ) approach, Comput. Phys. Comm. 238 (2019) 36–49.
[26] J.A. Warren, W.J. Boettinger, Prediction of dentric growth and microsegregation patterns in a binary alloy using the phase field method, Acta Metall. Mater. 43 (1995) 689–703.
[27] J. Zhao, Q. Wang, X. Yang, Numerical approximations for a phase field dendritic crystal growth model based on the invariant energy quadratization approach, Internat. J. Numer. Methods Engrg. 110 (2017) 279–300.
[28] C. Beckermann, H.-J. Diepers, I. Steinbach, A. Karma, X. Tong, Modeling melt convection in phase-field simulations of solidification, J. Comput. Phys. 154 (1999) 468–496.
[29] T. Takaki, Phase-field modeling and simulations of dendrite growth, ISIJ Int. 54 (2014) 437–444.